Presenting a Poster

ECE 4BI6

February 1, 2016

Overview of Poster

- It presents a story – your design project
- Includes an abstract giving a brief overview – what did you develop? why did you develop it?, what are the results or success?
- It includes a brief background of the approach – current technologies, relevant science
- It could include motivation – what patient groups, public, etc. are you trying to help
- It requires an overview (block or flow diagram)
- It can include specific component details if component is unique and interesting.
- It can include results
- It includes discussion and conclusions
- It can include references

Design Considerations

- Is it going to stand alone with no presenters present al the time to explain it?
- Is it going to be a background for presenter(s) describing and demonstrating the project?
- Is it going to be a combination of both?

General Rules

- Large text title and much smaller group names (authors) and their affiliation
- Poster information should have a natural or indicated flow
- Should be attractive with colour and some graphics effects (background)
- Should include a number of diagrams and figures
- Text blocks should be short and can be point form

Text or Font Selection

- Text must be readable at a distance of 6 to 8 feet
- Colour and background not too obtrusive
- Make sure text stands out in background (most pastel colours for text don’t work)
- Change font size or style to emphasize sections, important points, etc.

Figures

- Figures should be sufficient size so they can be easily viewed
- Should be necessary to the story
- Should be clear and not too detailed
- Should be labelled and captioned
- Include human element in figures

Combined Sensory Protection and Electrical Stimulation Improves Functional Outcomes of Denervated Rat Muscle

Michael P. Willand[1], Michael Holmes[2], James R. Bain[3], Hubert de Bruin[1], Margaret Fahnestock[2]

[1]School of Biomedical Engineering, [2]Department of Psychiatry & Behavioural Neurosciences, [3]Department of Surgery (Division of Plastic Surgery), McMaster University

MCMASTER SCHOOL OF BIOMEDICAL ENGINEERING

1 Introduction

Poor muscle and nerve functional recovery after nerve damage is a serious clinical problem. Immediate surgical repair of the damaged nerves is the best option for recovery but is not always possible or successful. Long term denervation leads to severe muscle atrophy, coupled with a loss of muscle spindles, force, motor function and an increase in tissue collagenization and fibrosis. Due to these factors, functional recovery following delayed reinnervation is poor.

2 Motivation

Our previous work demonstrated that suturing a sensory nerve to the distal motor nerve stump (called sensory protection) significantly improves muscle weight, force, morphological and histological aspects as well as preserving muscle spindles (Bain et al, 2001). More recently, we have shown that one month of electrical stimulation of denervated muscle also significantly increases muscle weight, force, and fiber area. We hypothesized that the combination of sensory protection and electrical stimulation will enhance functional recovery more than either of these treatments alone.

3 Methods

▪Surgeries and time points

Rat gastrocnemius muscles were denervated by cutting the tibial nerve. All animals had intramuscular electrodes implanted. The peroneal nerve was then sutured to the distal tibial stump following 3 months of treatment (electrical stimulation, sensory protection, or both). The muscles were allowed to recover for 3 additional months, and then functional measurements were taken and muscles excised for histological analysis.

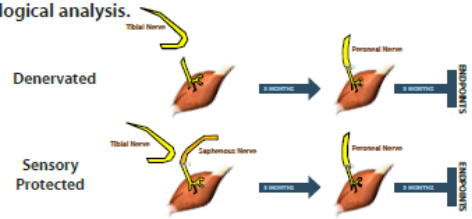

▪Neuromuscular electrical stimulation

Animals receiving stimulation were connected to a custom made stimulator and stimulated using a novel 1hr per day paradigm that was shown to be effective in denervated muscle (Willand et al, 2011).

▪Twitch and tetanic force measurement

Two needle electrodes were positioned in the belly of the muscle, connected to a stimulator, and the calcaneal tendon connected to a force transducer (Grass FD03). Muscle length was adjusted to the optimum length for force generation. Contraction and half-relaxation times were measured from the twitch force curves.

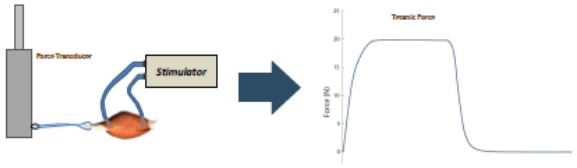

▪Motor unit number estimation (MUNE)

The number of motor units in each muscle was estimated using the incremental technique. Hook electrodes were placed on the peroneal nerve and recording electrodes placed in the muscle. Custom software written in LabVIEW used a wavelet based algorithm to characterize motor unit templates.

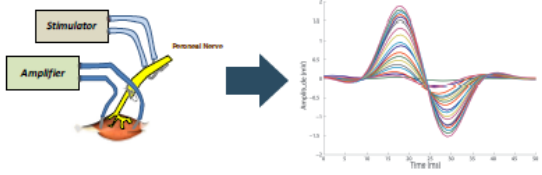

▪Histology and morphology

A rectangular sample from the belly of the medial gastrocnemius was extracted. 10µm sections were cut on a cryostat and stained for ATPase at pH 10. Samples were imaged using a Nikon D300 camera adapted to a Zeiss microscope and analyzed using ImageJ.

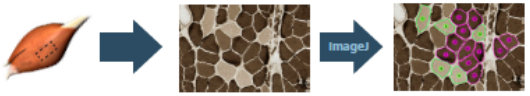

▪Statistics

A one way ANOVA was used for each endpoint measurement and if significant ($p<0.05$) a Tukey post-hoc test was used to compare groups. The contralateral leg in each animal served as a within animal control to minimize any variation due to different animal weights.

4 Results

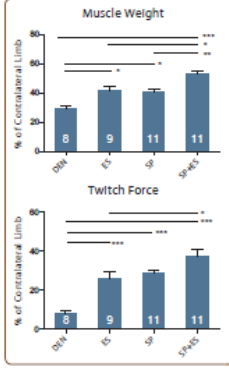

All treated groups had significantly greater measures compared to denervation alone. The combined treatment had significantly greater muscle weight than either treatment alone. Twitch force was also greater in the combined treatment. Sample size indictated in the bar.
(*p<0.05, **p<0.01,***p<0.001)

Legend
DEN: *Denervated*
ES: *Electrical Stimulation*
SP: *Sensory Protected*
SP+ES: *Sensory Protected Stimulated*

error bars in all graphs represent standard error of the mean

Motor unit counts were significantly greater in the combined treatment compared to sensory protection or denervation alone. There was no difference in counts between electrically stimulated and sensory protected stimulated animals

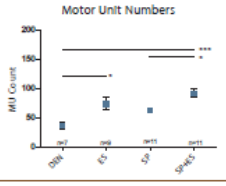

Contraction and half-relaxation times were no different between groups ($p>0.05$). Histological evaluation showed that stimulation alone significantly increased the size of type I fibers.

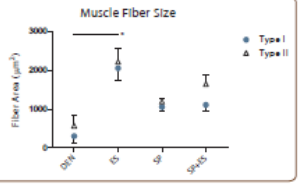

5 Conclusions

- Electrical stimulation combined with sensory protection significantly reduces atrophy and improves functional measures following delayed nerve repair, suggesting these approaches work through different mechanisms.
- The use of the combined therapy may provide new options for clinical treatment of denervated muscle.

References

Bain, J.R. *et al. Neuroscience* 103, 503-510 (2001).
Willand, M.P. *et al. J. Med. Biol. Eng.* 31, 87-92 (2011).

CIHR IRSC

Application of Wavelet Based Denoising Techniques to rTMS Evoked Potentials

Phil Chrapka, Supervisor: Dr. Hubert de Bruin

Department of Electrical and Computer Engineering, McMaster University

Introduction

Repetitve transcranial magnetic stimulation (rTMS) is currently used as a treatment for major depression. By stimulating the dorsolateral prefrontal cortex (DLPFC) one can affect deeper regions of the brain responsible for regulating an individual's mood.

Objectives

- Develop a technique that would use brain evoked potentials (EPs) to determine the optimum amplitude, stimulus site and frequency to increase the efficacy of rTMS
- Requires ability to record and analyze short to medium latency EPs (within 30ms post stimulus) to determine cortical sensitivity at the stimulation site
- Current clinical practice estimates the stimulus amplitude over the motor cortex which is determined by the cortical sensitivity of the motor cortex not the DLPFC and the subliminal excitability of the lower motor neuron pool
- Studying cortical EPs is difficult. There is a large compound muscle action potential (CMAP) that occurs within the first 30ms post stimulus.

Wavelets

- EPs are transient events and are ill suited for Fourier based analysis
- Wavelets offer the ability to localize transient events in time and frequency
- Wavelet transform (WT) is described by

$$W_\psi\{x\}(a,b) = \int_{-\infty}^{\infty} x(t)\psi^*_{a,b}(t)\,dt \qquad (1)$$

Wavelet Denoising

- Decomposes signal $x(t)$ into coefficients, through wavelet decomposition
- Modifies coefficients produced by (1) based on a certain threshold using shrinkage functions
- Reconstructs the signal with the new coefficients

Original Response

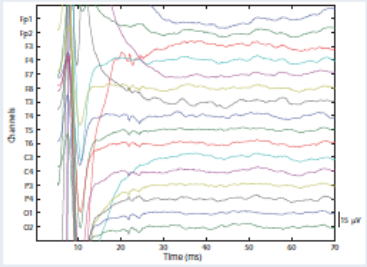

- Subject's response to 80 pulses of rTMS at 10Hz to the left B10 Brodmann area
- CMAP is present for the first 30ms of the response
- Cortical responses can be seen around 23ms
- Typical signal to noise ratio of patient responses is -44dB

Digital Filtering

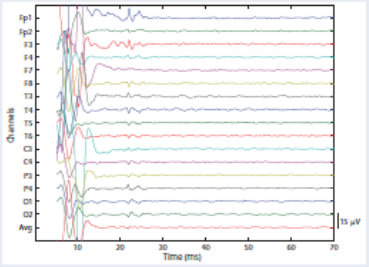

- Digital filter: zero phase 60th order Chebyshev filter, bandpass 150Hz-2kHz
- Successfully removed baseline fluctuations and limited the CMAP to the first 15ms
- The magnitude of the CMAP is still significantly larger than the remaining signal, making analysis of the 5-15ms region difficult

Residual of Wavelet Denoising with Soft Thresholding

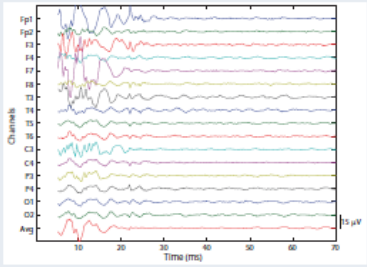

- CMAP is greatly attenuated within the first 15ms
- Signal after 20ms is similar to digital filtering results but retains more lower frequency activity

Residual of Wavelet Denoising with Hard Thresholding

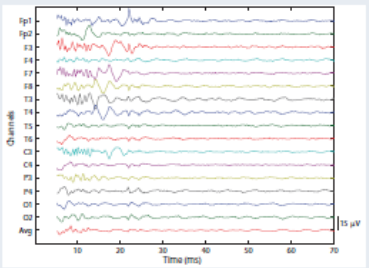

- Greater attenuation of the CMAP in comparison to the other two methods
- Brings out high frequency activity in left sided channels closer to the stimulation location (Fp1, F3 and F7)
- High frequency activity in the C3 channel is interesting because of its distance from the stimulation site

Current Method

- Digital filtering with a bandwidth of 150Hz-2kHz
- Can only reliably analyze EPs occurring after 13ms

Shrinkage Functions

$$\delta^{\text{soft}}(c_j) = \begin{cases} sgn(c_j)\left(|c_j| - \lambda_j\right), & |c_j| > \lambda_j \\ 0, & |c_j| \le \lambda_j \end{cases} \qquad (2)$$

$$\delta^{\text{hard}}(c_j) = \begin{cases} c_j, & |c_j| > \lambda_j \\ 0, & |c_j| \le \lambda_j \end{cases} \qquad (3)$$

where λ_j is the threshold at level j and c_j represents the wavelet coefficients at level j.

Proposed Method

1. Determine thresholds from sham recordings
2. Apply the WT to decompose the signal (5 levels, Daubechies wavelet with 4 vanishing points)
3. Apply the thresholds using soft or hard thresholding ((2) and (3), respectively)
4. Apply the inverse WT to reconstruct the signal using the modified wavelet coefficients
5. Calculate the residual by subtracting the denoised signal from the original signal

Conclusions

- Wavelet denoising methods are more effective than digital filtering
- Soft thresholding
  - Retains components of the CMAP whose amplitudes are limited to remain within the threshold
  - Assumes a worst case contribution from the cortical response
- Hard thresholding
  - Eliminates all components that exceed the threshold
  - Higher probability that remaining components result from cortical activity

References

[1] P. Chrapka, H. de Bruin, G. Hasey, "Application of Wavelet Based Denoising Techniques to rTMS Evoked Potentials." *Conf Proc IEEE Eng Med Biol Soc*, vol. 2012.

McMaster University

St. Joseph's Healthcare Hamilton

Dorsolateral Prefrontal Cortex Sensitivity to rTMS

Hubert de Bruin[1], Gary Hasey[2], and Julie Hemily[1]
[1]Department of Electrical and Computer Engineering, [2]Department of Psychiatry & Behavioural Neurosciences, McMaster University

McMaster University

ELECTRICAL AND COMPUTER ENGINEERING

1 Introduction

There has been considerable interest in the immediate effects of repetitive transcranial magnetic stimulation (rTMS) on post stimulus EEG and event related potentials (Thut and Pascual-Leone , 2010). Recently rTMS has been used to treat neuro-psychiatric disorders such as depression by stimulating the left or right dorsolateral prefrontal cortex (DLPFC) with high (>1Hz) and low (1Hz or less) rates respectively. To determine the patient specific cortical sensitivity a coil is placed on the scalp over the motor cortex and the underlying cortical tissue excited to find the lowest energy capable of inducing a compound action potential (CMAP) from a hand muscle, called the motor threshold (MT). Since there are no immediate recordable results such as the CMAP for the DLPFC, 80 to 120% of the MT is chosen as the stimulation energy for this area. For the treatment of depression the stimulus site is chosen by convention to be 5 cm anterior on a sagittal plane from the location of MT. This poster presents preliminary results of a study to determine DLPFC sensitivity of the three DLPFC areas suggested for treatment of depression, Brodmann areas 09, 10 and 46 using immediate brain responses.

2 Motivation

Cortical responses are very dependent on the stimulus site with some sites even having no or very limited responses, even the motor threshold varies considerably intra-subject from session to session, and prefrontal and motor cortices have different reactivity to TMS. The optimum stimulation current direction can also vary by at least 45° among subjects and each additional millimeter of distance between the cortex and coil increases the MT by approximately 2.8%. A common treatment protocol could therefore be suboptimal or ineffective for many patients who would otherwise benefit from rTMS. To determine successful DLPFC stimulation, immediate brain evoked potentials (EP), or event related potentials (ERP) could potentially have value in "personalizing" treatment site and stimulus energy.

3 Methods

▪Data Collection

SUBJECTS

Sixteen normal volunteers were used for the study

Ages 19-59
mean 33.2 ± 14.6

Each subject wore ear plugs and was instrumented with 16 fully notched recording gold cup electrodes in the 10-20 configuration (no central electrodes) with linked ear reference.

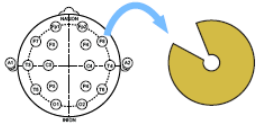

STIMULATION SITE LOCATION

MRI images were obtained for each subject and used with a stereotactic system to locate the cortical stimulation sites, electrode locations and reference the stimulating coil position to the stimulation site. Thresholds (MT) for the left and right motor cortex were obtained using the conventional technique. Stimulus site was chosen as the middle part of Brodmann area 46 (B46).

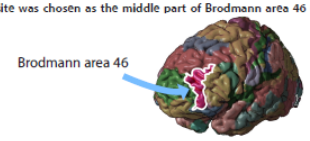

STIMULATION PARADIGMS

- Sequences of 40, 60 and 80 stimuli were delivered at 10 Hz with sham or 110% of MT to left B46.
- Sequences of 60 pulses were delivered at 1 Hz with sham, 90, 100 and 110% of MT to right B46.
- Sham rTMS stimulation used a passive coil held at B46 and an active coil held approximately 1 m away set at 60% of maximum energy to give the acoustic clicks.

RECORDING

Responses were recorded by a custom built EEG system, bandwidth .16 Hz to 2 kHz, at 5 kHz sampling rate and ensemble averaged in real time. The system locked out the amplifiers, using sample and hold circuitry (de Bruin et al., 2009), for 3.0 ms with the magnetic pulse given at 1 ms.

▪Post Processing

Averaged responses were digitally bandpass filtered using a zero-phase shift Chebyshev filter from 150 Hz to 2 kHz to ensure a zero baseline and remove some residual stimulus artifact and the very large (mV) muscle evoked M-waves recorded from primarily the temporalis muscle.

EP features chosen were total average channel signal power in windows 10 – 35 ms (EP) and 35 - 70 ms (background) similar to GMFA (Komssi et al, 2002).

4 Results

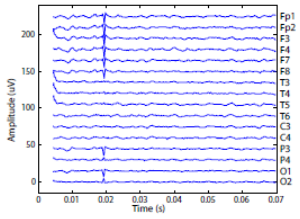

ACOUSTIC RESPONSES

Response of a 53 year old male to 80 pulses of 10 Hz sham stimulation with coil at left B46. Auditory responses were observed for most subjects for both left and right sham and true stimulations. True stimulations modulated the corresponding sham results. Acoustic responses were highly correlated suggesting volume conduction from deeper structures.

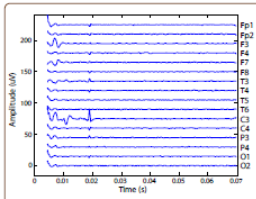

Response of a 19 year old female to 80 pulses at 10 Hz to left B46.

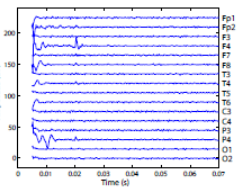

Response of a 21 year old female to 60 pulses at 1 Hz to right B46.

TRUE RESPONSES

Brain responses in bandwidth showed evoked potentials and modulated acoustic responses for both left and right stimulation. There was no evidence of short latency trans-callosal conduction for DLPFC stimulation in contrast to motor cortex stimulation. True responses were uncorrelated showing little volume conduction effects.

STUDY RESULTS

Each window average power was divided by the corresponding sham power to compensate for auditory and averaging noise.

- There was considerable variation in the individual responses to 110% MT 40, 60 and 80 stimuli delivered at 10 Hz to left B46, with no significant change in cortical responses with increasing number of stimuli.
- For right sided 90% and 110% MT stimulation a paired t-test showed a significant ($p < .01$) increase in average power ratios for the 10 – 35 ms EP window from 1.95 to 2.82.
- Average ratios for the EP window for the left and right sides were 3.76 and 2.82 respectively. With the left median significantly larger than the right ($p < .05$) using a Wilcoxon matched pairs test.

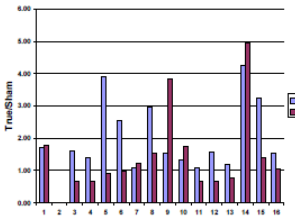

Left side background window average ratio was larger than right, 3.34 vs 1.50 and the left median was significantly higher than the right ($p < .05$) using a Wilcoxon one-tailed matched pairs test.

5 Conclusions

- EPs can be measured for the first 20 to 30 ms post stimulus, a window mostly ignored in other studies.
- Left sided 10 Hz stimulation at 110% MT results in larger cortical responses than for right sided at 1 Hz.
- Left sided stimulation at 10 Hz results in higher background activity while right sided 1 Hz stimulation reduces the activity below sham levels for many subjects as hypothesized.

References

Thut GR and Pascual-Leone A, *Brain Topogr.* **22**, 219-213 (2010)
de Bruin H et al. *Proc. (Biosignals) Biostec 2nd Int. Joint Conf. Biomed. Eng. Syst. & Techn*, 265-272 (2009)
Komssi S et al., *Clin. Neurophysiol.*, **113**, 175-184 (2002)

Using Short Latency Magnetically Evoked EEG Potentials to Determine the Prefrontal Region where 10 Hz Transcranial Magnetic Stimulation Induces the Greatest Cortical Response

Gary M. Hasey[1], Hubert de Bruin[2], Duncan MacCrimmon[1]
[1]Psychiatry and Behavioural Neuroscience, [2]Electrical and Computer Engineering
McMaster University, Hamilton, ON, Canada

McMaster University

Abstract

Repetitive transcranial magnetic stimulation (rTMS) is an effective treatment for major depressive disorder (MDD). Current protocol uses a stimulus position that is a fixed distance and orientation from the motor area for the abductor pollicis brevis, rather than a position determined by the subject's anatomy. This study stimulated the left dorsolateral prefrontal cortex at Brodmann areas 9, 10 and 46, as determined by each subject's MRI image. Responses were recorded for 70 ms during each 8 second train of 10 Hz stimulation and averaged using a custom EEG system. Short Latency magnetic evoked potentials (SL-MEPs) during 12 to 29 msec post stimulus were analyzed to determine cortical sensitivities for the three areas. Left hemisphere EPs for BA 10 and BA 46 were found to be statistically larger than for BA 9 using both signal power and GMFA (global mean field amplitude) for this time window.

Background

There is very good evidence that the cortical responses are very dependent on the stimulus site with some sites even having no or very limited responses [1]. It has also been found that even the motor threshold varies considerably intra-subject from session to session [2] and prefrontal and motor cortices have different reactivity to TMS [3]. The optimum stimulation current direction can also vary by at least 45° among subjects [4]. Finally the distance between the cortex and coil (scalp surface) has been found to be very important with an increase of ~2.8% in the motor threshold for each additional millimeter [5]. Recently, a clinical study reported that more lateral and prefrontal coil locations had better antidepressant responses [6].

Methods

Data Collection

Subjects

16 normal volunteers with no known neurological/ psychiatric deficits

Ages 19-59
mean 33.2 ± 14.6

Each subject wore ear plugs and was instrumented with 16 fully notched gold cup electrodes in the 10-20 configuration (no central electrodes) with linked ear reference

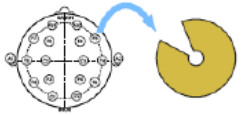

Stimulation Site and Paradigm

- MRI images were obtained for each subject and used with a stereotactic system to locate cortical stimulation sites and position the coil.
- Stimulus site was chosen as middle of each Brodmann area BA 9, BA 10 and BA 46.
- Sham and true stimulation for 8 sec at 10 Hz at 110% of motor threshold.

Recording and Signal Processing

- Data hardware filtered from .16 Hz to 2 kHz and sampled at 5 kHz.
- Digitally filtered from 150 Hz to 2 kHz (zero phase shift) to remove residual artifact and evoked M-waves from stimulated temporalis and occipitofrontalis muscles.
- Channels were re-referenced to average of all channels.
- SL-MEP features (total RMS channel power and GMFA [1]) were calculated for windows 12 to 29 ms and 29 to 70 ms for left hemisphere and both hemispheres
- Features normalized by sham values to minimize effect of brain responses to coil click.

Results

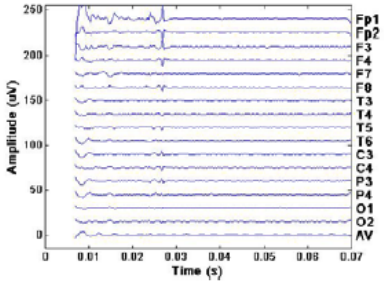

Fig. 1 Response of 26 year old female to stimulation of left BA 10

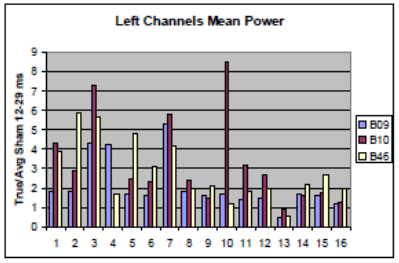

Fig. 2 Study Results for all subjects with mean power for left channels normalized by sham response power

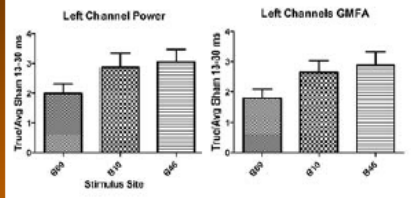

Fig. 3 Summary results (**Mean + SEM**) for all subjects for normalized left mean power and GMFA . The feature values for BA 46 and BA 10 are significantly greater than for BA 09, but not significantly different from each other (Kruskal-Wallis test $p < .05$; preplanned paired t-tests $p < .01$).

Discussion and Conclusions

- The custom EEG system allows us to record short latency magnetic evoked potentials from 3 to 4 msec post stimulus with no residual stimulus artifact.
- Bandpass filtering from 150 Hz to 2 kHz reliably removed stimulated muscle M-waves only from 12 msec post stimulus on for all three regions (muscle artifact especially prominent for BA 46 stimulation).
- Normalizing mean power and GMFA by the sham values accounts in part for residual background noise and the acoustic artifact resulting from the coil clicks (spikes at 27 msec in Fig. 1).
- Both normalized features convey the same information and represent the amplitude of the SL-MEPs relative to the sham response in the selected time window.
- Left hemisphere channel results are only shown here because there was little SL-MEP signal in the contralateral channels (e.g. Fig.1 where contralateral response is mostly acoustic artifact).
- Results for all 16 channels are similar except the differences are less significant.
- Greater cortical responses for BA 10 and BA 46 than for BA 9 help to explain the clinical results noticed in our lab and reported by Herbsman et al [6]
- Individual differences in cortical response (Fig. 2) suggest that SL-MEPs might be used to determine optimal treatment site for therapeutic rTMS

References:

[1] S. Komssi, H.J. Aronen, J. Huttunen, M. Kesäniemi, L. Soinne, V.V. Nikouline, M. Ollikainen, R.O. Roine, J. Karhu, S. Savolainen, and R.J. Ilmoniemi, " Ipsi- and contralateral EEG reactions to transcranial magnetic stimulation," *Clin Neurophysiol* vol 113, pp. 175-184, 2002.

[2] E.M. Wassermann, "Variation in the response to transcranial magnetic brain stimulation in the general population," *Clin Neurophysiol* Vol. 113 pp. 1165-1171, 2002.

[3] S. Kähkönen, J. Wilenius, S. Komssi and R.J. Ilmoniemi, "Distinct differences in cortical reactivity of motor and prefrontal cortices to magnetic stimulation", *Clin Neurophysiol*, vol. 115, pp. 583-588, 2004.

[4] D. Balslev, W. Braet, C. McAllister and R.C. Miall, "Inter-individual variability in optimal current direction for transcranial magnetic stimulation of the motor cortex", *J Neuroscience Methods*, vol. 162, pp. 309-313, 2007.

[5] M.G. Stokes, C.D. Chambers, I.C. Gould, T. English, E. McNaught, O. McDonald and J. Mattingley, "Distance-adjusted motor threshold for transcranial magnetic stimulation", *Clin Neurophysiol*, vol. 118, pp. 1617-1625, 2007.

[6] T. Herbsman, D. Avery, D. Ramsey, P. Holtzheimer, C. Wadjik, F. Hardaway, D. Haynor, M.S. George and Z. Nahas, "More lateral and anterior prefrontal coil location is associated with better repetitive transcranial magnetic stimulation antidepressant response", *Biol. Psychiatry*, vol. 66, pp. 509-515, 2009.

Assessment of Infant Movement Using Infant Accelerometer System

D. Gravem, M. Singh, C. Chen, J. Rich, J. Vaughan, B. Bodenhoeffer, S. Gallitto, M. Coussens, P. Chou , D. Cooper, D. Patterson
University of California, Irvine

INTRODUCTION

Assessing motor activity in neonates has achieved increasing importance, as there is mounting evidence that patterns of activity early in life can predict neuromotor impairments. Prechtl's General Movement's Assessment uses video observation of infants to identify abnormal movements predictive of Cerebral Palsy. In a study of 84 infants, the presence of these abnormal movements was 100% sensitive and 92% specific for CP at age 2. However, observation of physical activity is limited by observer skill, fatigue, and consistency. We have tested the use of a customized accelerometer system that consists of five 2g devices that can measure 3-axis of acceleration of the head and each of the 4 limbs. The device is wireless, gathers data every 200 msec and has an error rate of less than 0.3%. We hypothesized that this automated system would be useful in assessing motor activity in newborns.

METHODS:

10 preterm infants in the NICU were monitored for 1 hour using both the accelerometer system and video. Observers scored the infants for both quantity of movement (score of 1-4) or presence and absence of Cramped Synchronous Movements as defined by Prechtl's General Movement Assessment. The observer annotated the start and stop time for each abnormal infant movement. A Dynamic Bayesian Network was then trained to make the same assessment from acceleration-only data using 166 features from the data.

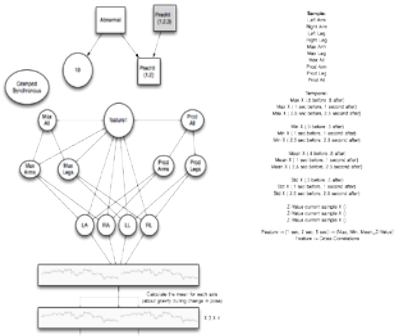

RESULTS:

The quantity of movement score matched our accelerometer algorithm 41% overall with 82.5%, 8.2%, 40.4%, and 53.0% for observer's scores of 1,2,3 and 4 respectively. The accelerometer was 100% in predicting the quantity of movement score +/- 1 category.

Six of the ten infants in the study exhibited Cramped Synchronous Movements, exhibiting a total of 102 abnormal movements during the monitoring. The accelerometer algorithm was 99% accurate in matching the observer's score for the presence or absence of cramped synchronous movements at any given time point during the 1 hour monitoring.

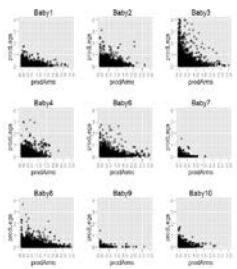

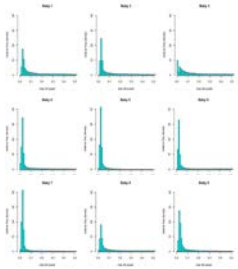

Quantity of Movement: Nurse Score vs. Accelerometer

Score	1	2	3	4
1	99	21	0	0
2	72	10	40	0
3	0	64	46	4
4	0	0	48	18

Prechtl General Movement: Nurse Score vs. Accelerometer

Total Number of Instances	55934	
Correctly Classified Instances	54540	97.5078 %
Incorrectly Classified Instances	1394	2.4922 %
	True Positive Rate	**False Positive Rate**
Cramped Movement	0.999	0.049
Non-Cramped Movement	0.951	0.001

CONCLUSIONS:

Early diagnosis of Cerebral Palsy and other motor disorders may lead to early treatment interventions for at-risk infants. Our initial observations comparing these two very different techniques suggest that the high data density accelerometer may prove useful as a clinical tool assessing abnormal patterns of motor activity in preterm infants.

Funded by: NIH Nursing Research,NR−09070

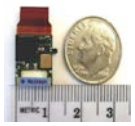

Novel Wearable Posture Correction Apparatus Using Advanced Accelerometry Techniques

Nanxi Zha and David Zhitomirsky, Electrical and Biomedical Engineering,
McMaster University

ABSTRACT

A novel posture correction apparatus was developed with the aim of stroke patient rehabilitation, specifically designed for patients with bodily neglect. The apparatus is based on an accelerometer system, capable of tracking tilt in three dimensions. The apparatus is portable and worn on the chest, and is extendable in design to other parts of the body. The approach to tilt sensing and posture correction taken here relies on small DC motor actuators implemented to notify the user of incorrect posture, based on their direction of tilt.

The design takes into account patient differences, and has calibration procedures to accommodate for different users and prevent sensor drift. Tilt is also continuously monitored on a remote computer, where signals from the accelerometer are transmitted wirelessly via a microcontroller and RF module. It was found that the system could reliably track tilt and thus posture, and the feedback mechanism was effective at notifying the user about incorrect posture.

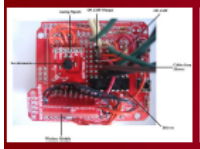

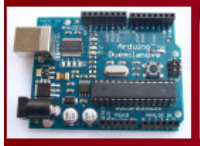

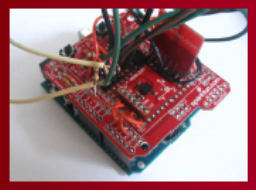

INTRODUCTION


Patients who are suffering from unilateral body neglect (e.g., as a result of a stroke) have a decreased awareness of a particular side of their body. Although they have trouble maintaining proper posture, corrections to their postures are possible when given encouragement (Punt, Riddoch 2006).

Currently, there are posture monitoring systems available involving accelerometers and gyroscopes (Hyde et al. 2008). This project will focus on the use of accelerometers due to their small size, light weight, and low cost (Mizuike, Ohgi & Morita 2009). Past accelerometer studies have been applied to posture maintenance and gait analysis. A series of accelerometers attached at the joints can model movements of the entire human body (Giansanti et al. 2003). By using frequency filtering and analysis techniques (e.g., Fourier Transform), the signals can be classified based on different posture (DC signals) and movement (AC signals) (Fahrenberg et al. 1997). It is believed that this posture correction system is a novel design in the rehabilitation and physiotherapy sciences. The resources used to implement this system are inexpensive but efficient. It allows for a portable system that can be applied to rehabilitation and physiotherapy.

MATERIALS AND DESIGN


ADXL355 Accelerometer

Figure 1. Overall Design


nRF24L01 Wireless Module


OPA2277 Operational Amplifier

Figure 2. Circuitboard Layout


Motors


Adruino Duomilanove Microcontroller


Figure 3. Wireless Implementation: Transmitter (top), Receiver (bottom)

Design of the tilt sensing apparatus involves using an accelerometer interfaced with a microcontroller, which is then interfaced with a feedback system.

The user is responsible for placing the posture correction system on their body and then assuming proper posture as outlined in this documentation or provided by a health professional. The system is responsible for tracking the user's tilt, and outputting appropriate feedback to notify the user of improper posture.

Software Setup: Data from the accelerometer was transmitted wirelessly via a nRF24L01 chip and an Adruino Microcontroller. This signal was then received by another nRF24L01 chip, an Adruino Microcontroller, which was connected to a laptop.


High Intensity LED

METHODS

Tilt implementation was done by interpreting acceleration along the axes as due to gravity.

Implementation algorithm is shown in figure 3, which involves tracking tilt angles and outputting appropriate feedback.

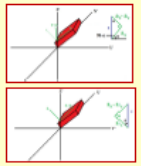
Figure 3. Tilt Angles

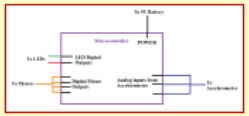
Figure 4. Microoontroller Layout


Figure 5. Tilt Sensing and Posture Correction

RESULTS

The tilt angles calculated from the tilt-sensing algorithm were tabulated and compared to the actual angle. This is seen in Figures 6 and 7.

Theoretical Angle (degrees)	Calculated Angle (degrees)	% Error
-90	-86.72	3.64444
-60	-58.91	1.81667
-30	-27.54	8.2
0	1.787	N/A*
30	30.57	1.9
60	62.19	3.65
90	85.25	5.27778

*N/A due to division by the theoretical value, which is zero

Figure 6. Theoretical vs. Calculated Angles (Left/Right Tilt)

Theoretical Angle (degrees)	Calculated Angle (degrees)	% Error
-90	-89.04	1.06667
-60	-56.76	5.4
-30	-26.96	10.1333
0	4.27	N/A*
30	28.95	3.5
60	66.03	10.05
90	86.08	4.35556

*N/A due to division by the theoretical value, which is zero

Figure 7. Theoretical vs. Calculated Angles (Forward/Backward Tilt)

It can be seen that the angle calculations are accurate. The biggest percent error is 10.1333%, with the majority of the percent errors under 5%. Therefore, the angle calculation equations are deemed to be accurate for this tilt application.

Figure 8 presents the LabVIEW user interface. The red dot represents the position of the accelerometer.

Corrective instructions are given as needed. Two fields are provided for adjustable tilt angle tolerances.

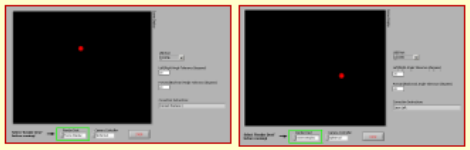
Figure 8. LabVIEW User Interface for Posture Modeling

DISCUSSION

Through vigorous testing, it can be seen that the implemented posture correction apparatus is successful in detecting improper posture. The device is capable of detecting left/right/forward/backward tilt, as well as tilt in any combination of these four directions. The wearable component can act stand-alone, while the LabVIEW tilt modeling component can be added on wirelessly.

For future considerations, additional accelerometers can be added for posture monitoring at different joints (E.g., the shoulders). Horizontal translation should be measured as well, in order to provide more posture information for the user. The LabVIEW user interface can be edited to be more user-friendly. The overall packaging of the device can be scaled down and be more aesthetically pleasing.

CONCLUSIONS

A robust and practical posture correction device has been constructed using accelerometer techniques. It was found that the accuracy of the system is sufficient to monitor posture, and the motors are an effective and way to provide feedback without irritating the subject. The current developed technology allows for pre-programmed tilt posture correction based on set algorithms, and wireless tilt visualization.


Figure 9. Front of Wearable Module (Left), Back of Wearable Module (Middle), Wireless Receiver Module (Right)

REFERENCES

Fahrenberg, J., Foerster, F., Smeja, M. & Muller, W. (1997), "Assessment of posture and motion by multichannel piezoresistive accelerometer recordings", Psychophysiology, vol. 34, no. 5, pp. 607-612.

Giansanti, D., Maccioni, G., Macellari, V., Macchini, G. & Cesareo, A. (2003), "Is it feasible to reconstruct body segment 3-D position and orientation using accelerometric data?", IEEE transactions on bio-medical engineering, vol. 50, no. 4, pp. 476-483.

Godfrey, A., Conway, R., Meagher, D. & Ólaighin, G. (2008), "Direct measurement of human movement by accelerometry", Medical engineering & physics, vol. 30, no. 10, pp. 1364-1386.

Hyde, R.A., Ketchiham, L.P., Neild, S.A. & Jones, R.S. (2008), "Estimation of upper-limb orientation based on accelerometer and gyroscope measurements", IEEE transactions on bio-medical engineering, vol. 55, no. 2 Pt 1, pp. 746-754.

Kavanagh, J.J. & Menz, H.B. (2008), "Accelerometry: a technique for quantifying movement patterns during walking", Gait & posture, vol. 28, no. 1, pp. 1-15.

Mizuike, C., Ohgi, S. & Morita, S. (2009), "Analysis of stroke patient walking dynamics using a tri-axial accelerometer", Gait & posture, vol. 30, no. 1, pp. 80-85.

Morris, J.R. (1973), "Accelerometry--a technique for the measurement of human body movements", Journal of Biomechanics, vol. 6, no. 6, pp. 729-736.

Punt, T.D. & Riddoch, M.J. (2006), "Motor neglect: implications for movement and rehabilitation following stroke", Disability and rehabilitation, vol. 28, no. 19-54, pp. 857-864.

ACKNOWLEDGEMENTS

This work was made possible under the guidance of Professor Hubert deBruin of McMaster University, who gave invaluable advice in regards to sensor implementation and system design.

McMaster University

Inspiring Innovation and Discovery

A System to Quantify Upper Limb Function

Larissa Schudlo, Natalie Tong
Supervisor: Dr. H. deBruin

Introduction

Peripheral nerve damage in the upper extremity can reduce a person's strength and range of motion, and must be immediately repaired. Post operative recovery must include a therapy program, and the assessment of motor function to ensure adequate rehabilitation. However, traditional assessments include qualitative or semi-quantitative evaluation techniques and can lead to inaccuracies [1]. Nerve injuries in the upper limb are prevalent in pediatric patients, which further increases the difficultly in providing an accurate assessment. A device that would allow clinicians to qualitatively assess a pediatric patient's grip strength and movement capabilities would improve the accuracy and reliability of evaluating rehabilitation.

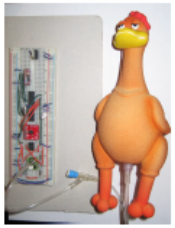

Fig.1: A squeeze toy instrumented with electronics to obtain quantitative grip force and range of motion measurements .

Motivation

The objective of this project was to design an instrumentation system that would quantify muscle function and improve the precision and reliability of rehabilitation assessment of the upper extremity (Figure 1). This instrumentation allows clinicians to measure and objectively evaluate patient recovery in the areas of force and range of motion. The system was particularly aimed toward pediatric patients rehabilitating from peripheral nerve damage. In order to achieve this goal, a device was developed that combines a biomedical engineering approach with the current clinical therapy assessment techniques being used.

References

1. G. Kurillo, M. Gergoric, N. Goljar, and T. Bajd, "Grip force tracking system for assessment and rehabilitation of hand function," *Tech. and Health Care*, vol. 13, pp. 137-149, 2005;
2. Y. Huang, K. Low, and H. Lim, "Objective and quantitative assessment methodology of hand functions for rehabilitation - closing the gap between clinical and engineering knowledge," *Proc. 2008 IEEE Intl. Conf. Robotics Biomimet.*, pp. 846-851, 2009.

Design

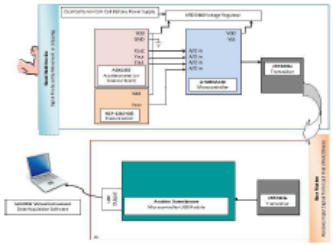

Fig.2: Block diagram of design components.

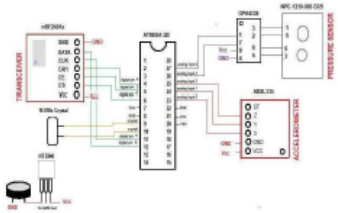

Fig.3: Schematic diagram of the design of electronics used to instrument the toy.

To develop the quantification system, a child's handheld toy was instrumented with the necessary transducers to capture force and range of motion. The data is measured and transmitted from the hand held device to a base station, then sent to a computer for evaluation. After the appropriate calculations are made using analysis software, the information is output on an interactive display to provide understandable, useful information about the patient's capabilities. This procedure is outlined in Figure 2.

Hand Held Toy

A pneumatic squeeze toy was instrumented with a gauge-type pressure sensor for the acquisition of grip force measurements, a three axis accelerometer for motion control and movement measurements, and additional electronics for signal acquisition and transmission. The pressure sensor compares the pressure within the toy to the ambient pressure of the environment. Thus, the pressure reading should be 0mmHg when the toy is at rest, and stronger exerted grip forces would result in larger pressure readings. The accelerometer was used to measure the extent which a patient can pronate and supinate their forearm, and the speed which these movements can be performed. When the patient performs these movements, the accelerometer readings are processed to determine the amount of tilt from initial position along its axis (anti-parallel to gravity), and the angular velocity of the movement.

The analog output signals from these transducers are sampled and digitized by a microcontroller, then sent to a transceiver. Using radiofrequency (RF) wireless communication to ensure patient safety and complete isolation from a power supply and ground, the data is then transmitted from the toy to the base station (Figures 3 and 4). Due to patient's limited muscle function, the hardware components are light yet measure the data with a high degree of sensitivity to ensure even minute movements and forces are captured.

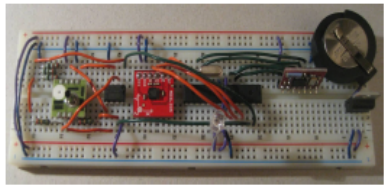

Fig.4 Completed electronic circuit to instrument toy.

Base Station

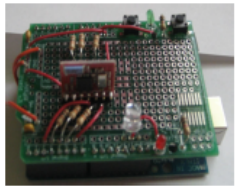

Fig.5: Completed electronic circuit for base station.

Acquired force and motion data transmitted from the handheld toy is received at the base station by another transceiver, and read in by another microcontroller (Figures 5 and 6). The microcontroller in the base station is part of an Arduino Duemilanove USB module. This module is powered through USB, and provides the necessary hardware to establish the USB-Serial port communication with the computer. Through this connection, the data is sent to data acquisition software on the computer.

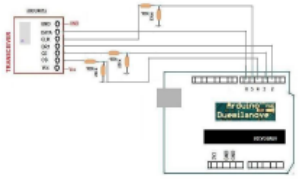

Fig.6: Schematic Diagram for design of electronics used in hand held toy.

Software

The software program used to process and display acquired transducer data was written in LabVIEW. This interactive program processes the data and displays it to the user. Upon starting the program, the user can navigate through to select which type of data will be evaluated in the current session (force or motion), and whether they will be viewing past patient history or recording new data. If the user selects to view past patient history, they can select the appropriate files to view past results and compare multiple sessions at once. If the user selects to record new data, new files are created in the appropriate location. Once the necessary files are created, the user can start recording new data. As the activity is performed, the information is displayed on the front panel and saved for future viewing.

Results

As the data is acquired, it is displayed on the front panel for the user to evaluate. Figure 7 shows the front panel of the designed software program when grip force data is acquired. Figure 8 shows the front panel of the designed software program when acceleration and rotation data is obtained.

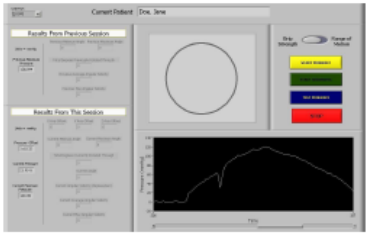

Fig.7: Front panel of software program, showing the acquisition of grip force measurements.

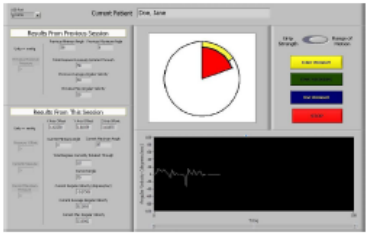

Fig.8: Front panel of software program, showing the acquisition of angular velocity and rotation measurements.

Conclusion

Through the instrumentation of a squeeze toy and the development of a user-friendly interface, grip force and motion measurements of children can be recorded and analyzed. With this quantitative information, physiotherapists are able to more effectively evaluate patient progression in rehabilitation therapy.

Acknowledgements

The authors would like to thank Dr. H. deBruin and Mike Willand for their advice and guidance throughout this project. We would also like to acknowledge Carol DeMatteo from McMaster's School of Rehabilitation Sciences, Tara Packham from the Mac Hand Therapy Program and Dr. Jamie Bain in the Brachial Plexus Clinic at the McMaster Children's Hospital for providing opportunities for project research and instrumentation specification, as well as Howie Keown of the Biomedical Technology Department at McMaster Medical Center for providing equipment and facilities used in this work.